Phase retrieval of diffraction patterns from noncrystalline samples using the oversampling method

Jianwei Miao*
Stanford Synchrotron Radiation Laboratory, Stanford Linear Accelerator Center, Stanford University, Stanford, California 94309-0210

Tetsuya Ishikawa
SPring-8/RIKEN, 1-1-1, Kouto, Mikazuki, Sayo-gun, Hyogo 679-5148, Japan

Erik H. Anderson
Center for X-ray Optics, Lawrence Berkeley National Laboratory, Berkeley, California 94720

Keith O. Hodgson
Stanford Synchrotron Radiation Laboratory and Department of Chemistry, Stanford University, Stanford, California 94305
(Received 16 August 2002; revised manuscript received 11 November 2002; published 14 May 2003)

We report the experiments and procedures to successfully record and reconstruct coherent diffraction patterns at sub-10-nm resolution from noncrystalline samples by using synchrotron x rays with a wavelength of 2 Å. By employing the oversampling phasing method, we studied the quality of image reconstruction of experimental diffraction patterns as a function of the oversampling ratio (a parameter to characterize the oversampling degree). We observed that the quality of reconstruction is strongly correlated with the oversampling ratio, which is in good agreement with theory. When the oversampling ratio is around 5 or larger, the reconstructed images with high quality were obtained. When the oversampling ratio is less than 5, the images became noisy. When the oversampling ratio is very close to or less than 2, the images were extremely noisy and barely recognizable. We believe these results will be of importance to the experiments of imaging nanocrystals and noncrystalline samples using coherent x-ray, electron, or neutron diffraction.

DOI: 10.1103/PhysRevB.67.174104 PACS number(s): 61.10.Eq

I. INTRODUCTION

X-ray crystallography is a well-established and widely used technique to determine the three-dimensional (3D) structures of crystalline materials at atomic resolution. The large number of unit cells inside a crystal produces strong and discrete Bragg peaks, which facilitates data acquisition but imposes the well-known ''phase problem.'' When a sample is noncrystalline, the diffraction patterns become weak and continuous, which makes the data acquisition more challenging. However, such a continuous diffraction pattern can be sampled at a spacing finer than the Bragg peak frequency (i.e., oversamples). Although it was suggested early that oversampling a diffraction pattern may provide phase information,[1,2] it was not until recently that a theory was proposed to explain the oversampling phasing method and confirmed by computer simulation.[3,4]

The first experimental demonstration of using the oversampling method to image noncrystalline samples was carried out in 1999.[5] Since then, a variety of applications of this methodology have been pursued, ranging from imaging the shapes of Au nanocrystals to theoretical studies of the potential of imaging single biomolecules using x-ray free-electron lasers.[6–15] In this paper, we describe the detailed experiments and procedures to record and reconstruct coherent diffraction patterns at sub-10-nm resolution. Furthermore, we studied the phase retrieval of experimental diffraction patterns as a function of the oversampling ratio, and the results are in agreement with theory.

The paper is organized as follows. In Sec. II, the basic theory of the oversampling method is reviewed. In Sec. III, the experimental instrument and the procedures to obtain high-quality diffraction patterns from noncrystalline samples using coherent x rays are discussed. Section IV describes the reconstruction of a high-quality image of a noncrystalline sample at 7-nm resolution, and the results of how the quality of image reconstruction depends on the oversampling ratio. Conclusions are presented in Sec. V.

II. THE OVERSAMPLING METHOD

When a coherent beam of x rays illuminates a sample with an electron density of $\rho(x,y,z)$, the diffraction pattern, if sampled at the Bragg peak frequency, is expressed as

$$|F(k_x,k_y,k_z)| = \left| \sum_{x=0}^{l-1} \sum_{y=0}^{m-1} \sum_{z=0}^{n-1} \rho(x,y,z) e^{2\pi i(k_x x/l + k_y y/m + k_z z/n)} \right|, \quad k_x=0,\ldots,l-1, \quad k_y=0,\ldots,m-1, \quad k_z=0,\ldots,n-1 \tag{1}$$

where $|F(k_x,k_y,k_z)|$ is the magnitude of the Fourier transform of the sample, and l, m, and n are the size of the sampling array in x, y, and z directions, respectively. According to Eq. (1), the phase problem becomes how to solve $\rho(x,y,z)$ from a series of nonlinear equations. When $\rho(x,y,z)$ is real, the number of unknown variables [i.e., the voxel number of the 3D array sampling $\rho(x,y,z)$] is lmn, and the number of independent equations is $lmn/2$ due to the centrosymmetry of the diffraction pattern. When $\rho(x,y,z)$ is complex, the number of unknown variables becomes $2lmn$, and the number of independent equations is lmn. In either

case, the number of unknown variables is twice the number of equations, and the phase information cannot be uniquely retrieved from the diffraction pattern without other information.[3,4]

When the diffraction pattern is sampled at a frequency of $\sqrt[3]{2}$ finer than the Bragg peak frequency, the magnitude of the Fourier transform becomes

$$|F(k_x,k_y,k_z)|=\left|\sum_{x=0}^{l-1}\sum_{y=0}^{m-1}\sum_{z=0}^{n-1}\rho(x,y,z)\times e^{2\pi i[k_x x/(\sqrt[3]{2}l)+k_y y/(\sqrt[3]{2}m)+k_z z/(\sqrt[3]{2}n)]}\right|,$$

$$k_x=0,\ldots,\sqrt[3]{2}l-1,\quad k_y=0,\ldots,\sqrt[3]{2}m-1,\quad k_z=0,\ldots,\sqrt[3]{2}n-1. \tag{2}$$

For real $\rho(x,y,z)$, the number of independent equations becomes lmn, while the number of unknown variables remains lmn. For complex $\rho(x,y,z)$, both the number of independent equations and the number of unknown variables are $2lmn$. In either case, there are as many independent equations as unknown variables. When the sampling frequency is finer than $\sqrt[3]{2}$, the number of independent equations is more than the number of unknown variables, and $\rho(x,y,z)$ can in principle be directly solved from the series of equations.[3] One may argue that it does not guarantee a unique solution to have more equations than unknown variables. Mathematically, it has been shown that the multiplicity of the solution is rare in two- and three-dimensional cases.[16]

Oversampling a diffraction pattern at a spacing finer than the Bragg peak frequency corresponds to surrounding the electron density of the sample with a non-density region. The finer the sampling frequency, the larger the no-density region. To characterize the oversampling degree, a concept called the oversampling ratio (σ) was introduced to define the oversampling degree[3]

$$\sigma=\frac{(\text{volume of electron density region})+(\text{volume of no-density region})}{(\text{volume of electron density region})}. \tag{3}$$

When $\rho>2$ (corresponding to the sampling frequency $>\sqrt[3]{2}$), the no-density region is larger than the electron density region, and the phase information can in principle be directly retrieved using an iterative algorithm.[3,4,17,18] Note that the discussion above only deals with the Fraunhofer approximation (i.e., far-field diffraction). In the Fresnel approximation (i.e., near-field diffraction), the phase problem is intrinsically different and a potential approach is to use the transport of intensity method.[19]

III. EXPERIMENT

The experiments reported herein were carried out using an undulator beamline at SPring-8.[20] An imaging instrument was mounted at a distance of 59 m from the center of the undulator. Figure 1 shows the schematic layout of the chamber. The first element inside the chamber was a 20-μm pinhole mounted on an in-vacuum motorized stage. An **L**-shaped guard slit, placed 25.4 mm downstream of the pinhole, was used to eliminate the scattering from the edge of the pinhole. The combination of the pinhole and the **L**-shaped guard slit generated three clean quadrants and one noisy quadrant on the detector. The diffraction patterns in the noisy quadrant were recovered by using the centrosymmetry of the diffraction patterns, which is due to the fact that the electron density of samples is usually real in the hard-x-ray region. At a distance of 12.7 mm away of the **L**-shaped guard slit was a sample holder, which can rotate samples in 360° for recording 3D diffraction patterns. A charge-coupled device (CCD) detector was placed downstream of the sample holder at a distance of 743 mm. The distance (x) between the CCD and the sample is determined by

$$\frac{\lambda}{Oa}=\frac{\Delta y}{x}$$

and

$$O=\begin{cases}\sqrt{\sigma} & \text{for a 2D sample with size of } a\times a\\ \sqrt[3]{\sigma} & \text{for a 3D sample with size of } a\times a\times a\end{cases}, \tag{4}$$

where λ is the x-ray wavelength and Δy the pixel size of the CCD detector. The CCD detector is a deep depletion and direct illumination detector with 1152×1242 pixels and a pixel size of 22.5×22.5 μm. The estimated quantum efficiency of the CCD detector is about 77% for 2 Å x rays. The CCD detector was mounted on a motorized X-Y stage and could be shifted ±25.4 mm in both X and Y directions for recording higher-resolution diffraction patterns. In front of the CCD detector was a beam stop to block the direct beam

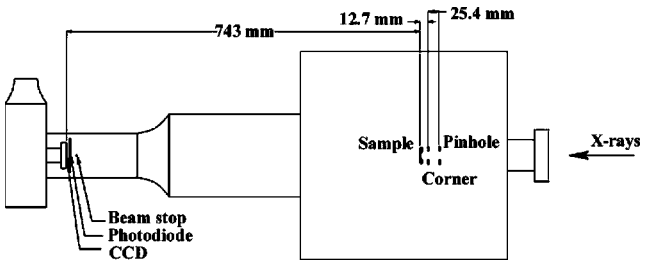

FIG. 1. Schematic layout of the experimental instrument used for the recording of the coherent x-ray diffraction patterns.

and a photodiode to align the pinhole, the **L**-shaped guard slit and the sample. All the elements were in vacuum with a pressure of $\sim 10^{-6}$ Torr.

The oversampling method is strongly correlated with the coherence of the incident x rays. Since oversampling a diffraction pattern corresponds to surrounding the structure of a sample with a no-density region, the coherence length of the incident beam should be larger than the overall size of the sample and the no-density region. The higher the oversampling degree, the finer of the correspondingly features of the diffraction pattern have to be recorded faithfully, and hence the larger the coherence length of the incident beam needs to be. The required spatial and temporal coherence of the incident x rays are related to the oversampling degree by

$$\frac{\lambda}{\Delta\lambda} \geqslant \frac{Oa}{d}, \quad \Delta\theta \leqslant \frac{\lambda}{2Oa}, \tag{5}$$

where d is a desired resolution, and $\Delta\theta$ the divergence or convergence angle of the incident x rays. Based on Eqs. (5), the required coherence for this setup was estimated to be $\lambda/\Delta\lambda > 943$ and $\Delta\theta < 1.5\times 10^{-5}$ rad for a desired resolution of 7 nm. At the SPring-8 beam line, a Si(111) double crystal was used to achieve the temporal coherence of $\lambda/\Delta\lambda \sim 7500$.[20] While the vertical spatial coherence of the undulator beam was better than that required, the needed horizontal spatial coherence was achieved by placing a 150-μm slit at a distance of 27 m upstream of the instrument.

IV. RESULTS AND DISCUSSION

With the instrument described above, we have recorded diffraction patterns from a noncrystalline sample by using coherent x rays with a wavelength of 2 Å. The sample, made of Au, consists of a single layered pattern with a size of $2.5\times 2\times 0.1$ μm and was supported by a silicon nitride membrane window, which is transparent to x rays. Figure 2(a) shows a scanning electron microscopy (SEM) image of the sample. In order to obtain a high-resolution diffraction pattern, we shifted the CCD detector in both *X* and *Y* directions to record a set of diffraction patterns at different resolution and then tiled them together. Figure 2(b) shows a diffraction pattern with 2000×2000 pixels and a resolution of 7 nm at the edge. The exposure time of the diffraction pattern is about 50 min with an unfocused undulator beamline. Since the beam stop was used to block the direct beam, the diffraction pattern has a missing data area at the center with a size of 60×60 pixels.[21] We filled in the missing data area by a patch of the diffraction pattern calculated from a soft-x-ray microscopy image of the sample.[22,23]

To retrieve the phase information from oversampled diffraction patterns, an iterative algorithm has been used of which the *j*th iteration consists of the following seven steps.

(i) A temporary Fourier transform was calculated by

$$F'_j(k_x,k_y,k_z) = |F_{\text{expt}}(k_x,k_y,k_z)|e^{\varphi_{j-1}(k_x,k_y,k_z)}, \tag{6}$$

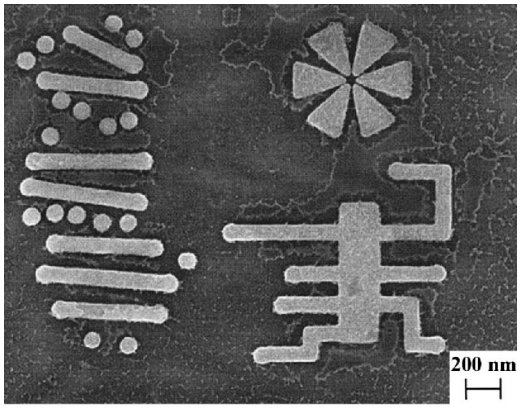

(a)

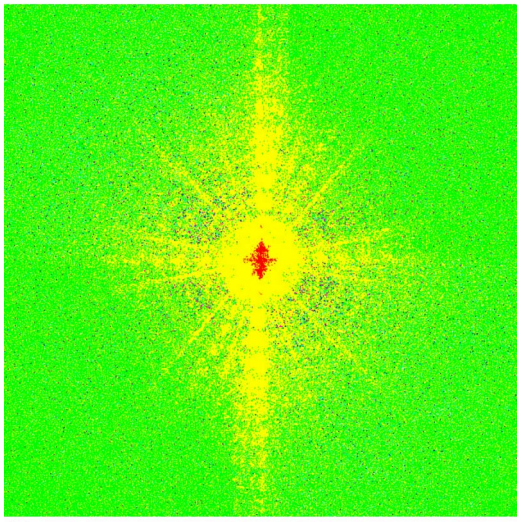

(b)

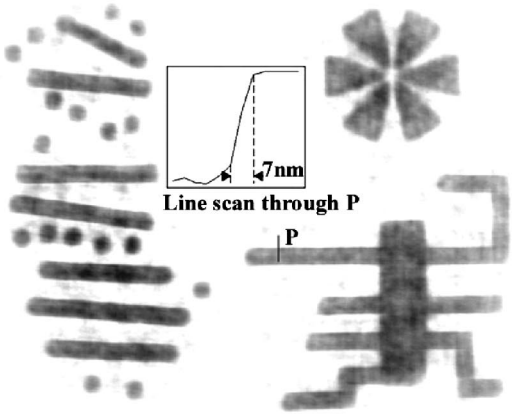

(c)

FIG. 2. The recording and reconstruction of a diffraction pattern from a noncrystalline sample by using coherent x-rays with a wavelength of 2 Å. (a) A SEM image of a noncrystalline sample made of Au. (b) A high-resolution diffraction pattern (a 2000×2000 pixel array) recorded from the sample (displayed in a logarithmic scale). (c) The structure of the sample reconstructed from (b) in which a line scan through an edge shown in the inset demonstrates the resolution of 7 nm.

where $\varphi_{j-1}(k_x,k_y,k_z)$ represents the phases of the Fourier transform at the $(j-1)$th iteration and $|F_{\exp}(k_x,k_y,k_z)|$ is the measured magnitude of the Fourier transform.

(ii) $\varphi'_j(0,0,0)$, the phase of $F'_j(0,0,0)$, was set to 0 due to the centrosymmetry of the diffraction pattern.

(iii) A temporary electron density, $\rho'_j(x,y,z)$, was computed from $F'_j(k_x,k_y,k_z)$ by using an inverse fast Fourier transform (FFT).

(iv) To monitor the convergence of process, a normalized error function (γ) was used in each iteration

$$\gamma=\frac{\sum_{x,y,z\notin S}|\rho'_j(x,y,z)|}{(\sigma-1)\sum_{x,y,z\in S}|\rho'_j(x,y,z)|}, \tag{7}$$

where S is the finite support and γ represents the averaged error per pixel that is independent of the oversampling ratio.

(v) A new electron density was obtained by

$$\rho_j(x,y,z)=\begin{cases}\rho'_j(x,y,z) & \text{if } (x,y,z)\in S \text{ and } \rho'_j(x,y,z)\geqslant 0\\ \rho_{j-1}(x,y,z)-\beta\rho'_j(x,y,z) & \text{if } (x,y,z)\notin S \text{ or } \rho'_j(x,y,z)<0\end{cases} \tag{8}$$

where β, a constant to adjust the convergence process, was set to 0.9 in all the reconstructions.

(vi) A new Fourier transform, $F_j(k_x,k_y,k_z)$, was calculated from the new electron density of $\rho_j(x,y,z)$ by using FFT.

(vii) The phase set, $\varphi_j(k_x,k_y,k_z)$, was used for the next iteration.

By using the iterative algorithm with a random phase set as an initial input and a 2.53×2.06 μm square as the finite support (which corresponds to $\sigma=9.4$), we recovered the phase information for the diffraction pattern shown in Fig. 2(b). Figure 2(c) shows the reconstructed image with a resolution of 7 nm, in which both the shapes of individual nanostructures and the variation of the electron density inside the nanostructures are visible. We performed five more reconstructions with different initial random phase sets and the detailed features in the reconstructed images were consistent. We then studied the quality of image reconstruction as a function of the oversampling ratio (σ). We first converted the diffraction pattern of Fig. 2(b) to a 1460×1460 pixel array by binning pixels where we assumed that each pixel has a finite area and the pixel value is uniformly distributed inside the area. The new diffraction pattern has the same spatial resolution, but a lower oversampling ratio of $\sigma=5$ for a 2.53×2.06-μm finite support. By using a random phase set as an initial input, we reconstructed the electron density of the sample after about 2000 iterations, shown in Fig. 3(a). The white area in Fig. 3(a) represents the no-density region, which is due to the oversampling of the diffraction pattern, and the square in dotted line shows the finite support. We carried out four more trials with different random initial phase sets, and the reconstructed images were consistent and successful, while the iteration number varied in each case. We further reduced the sampling frequency of the diffraction pattern of Fig. 2(b) to a 1308×1308 pixel array, which corresponds to $\sigma=4$ for the same 2.53×2.06-μm finite support. Figure 3(b) shows a reconstructed image with the quality inferior to that of Fig. 3(a). We have performed four more trials with different initial random phase set, and the quality of the reconstructed images is comparable to that of Fig. 3(b). We continued to reduce the sampling frequency of the diffraction pattern to an 1132×1132 pixel array, corresponding to $\sigma=3$ for the same finite support. We have carried out five reconstructions with different initial random phase sets. While the reconstructed images are recognizable, they are noisy, as Fig. 3(b) shows. Finally, the diffraction pattern of Fig. 2(b) was converted to a 924×924 pixel array, which corresponds to $\sigma=2$ for the same finite support. We have carried out five reconstructions, and the reconstructed images are extremely noisy and barely recognizable, shown in Fig. 3(d).

Figure 4 shows the normalized error function versus the iteration number in which curves *a*, *b*, *c*, and *d* correspond to the reconstructions of Figs. 3(a), 3(b), 3(c), and 3(d), respectively. By comparing curves *a*, *b*, and *c*, one can see that the normalized error function indeed indicates the quality of the reconstructions. An interesting observation is that curve d converged to a number smaller than that in curves *a*, *b*, and *c*. This is because, when σ is less than or very close to 2, there are no unique phase sets in the diffraction pattern. Although the algorithm converged to a phase set which is a solution to the equations, it is actually an incorrect phase set.

The results of the studies agree with the theoretical explanation illustrated in Sec. II. When the oversampling ratio σ is much larger than 2, the number of equations is far more than the number of unknown variables. This redundancy makes it easier to retrieve the phase information directly from the diffraction pattern. However, when σ approaches 2, there is slight difference between the theory and the results of the studies. From theory, we concluded that, as long as $\sigma>2$, there is a unique phase set available from the diffraction pattern itself. However, the studies of the experimental diffraction pattern showed that, when σ is close to 2, the reconstructed image becomes quite noisy. We believe this is due to (i) the noise in the experimental diffraction pattern and (ii) the algorithm becoming trapped in a local minimum instead of converging to the global minimum. With the presence of noise in the diffraction pattern, the intensity points with low

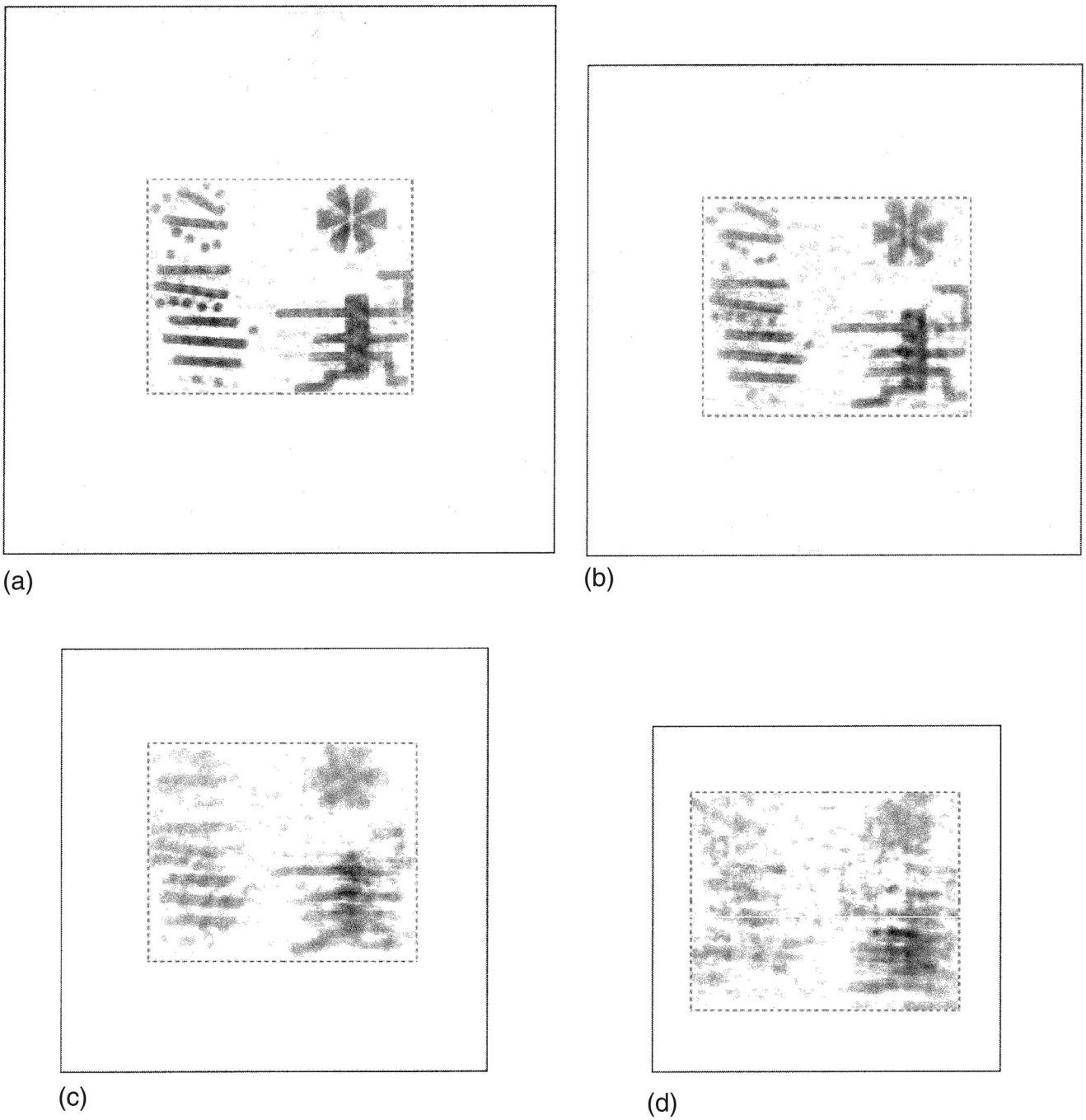

FIG. 3. Phase retrieval of an experimental diffraction pattern as a function of the oversampling ratio (σ). (a) A reconstructed image with $\sigma=5$ where the white area represents the no-density region, and the square in dotted line is the finite support 2.53×2.06 μm. (b) A reconstructed image with $\sigma=4$. Note that the white area becomes smaller. (c) A reconstructed image with $\sigma=3$. (d) A reconstruction image with $\sigma=2$.

signal-to-noise ratio are somewhat smeared out, which actually reduces the number of independent equations. Secondly, when the number of unknown variables is close to the number of independent equations, the algorithm is very easily trapped in a local minimum instead of the globe minimum. This has been observed in our previous studies of phase retrieval as a function of σ using simulated diffraction patterns.[3]

V. CONCLUSIONS

Using coherent x rays with a wavelength of 2 Å from a synchrotron undulator beamline and a specially designed instrument, we have measured high quality continuous diffraction patterns from a noncrystalline sample. By employing the oversampling phasing method, a coherent diffraction pattern has been successfully converted to a real space image with a resolution of 7 nm. By studying the quality of image recon-

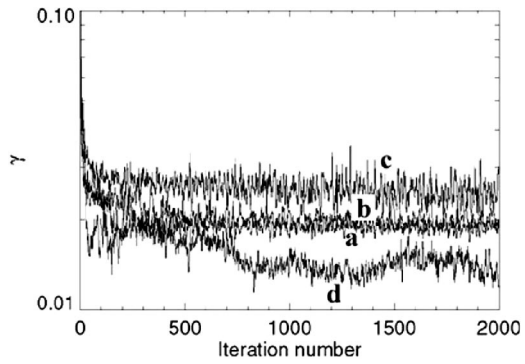

FIG. 4. The normalized error function vs the iteration number. Curves *a*, *b*, *c*, and *d* correspond to the reconstruction with $\sigma=5$, $\sigma=4$, $\sigma=3$, and $\sigma=2$, respectively.

struction of an experimental diffraction pattern as a function of the oversampling ratio (σ), we verified they are indeed strongly correlated. When σ is close to 5 or larger, good quality reconstructed images were obtained.[24] When σ is less than 5, the images were noisy. When σ is very close to or less than 2, the reconstructions were not successful at all. Although these studies were carried out using a 2D x-ray diffraction pattern, we believe the results can in principle be generally extended to 2D and 3D coherent diffraction imaging using x-rays, electrons or neutrons.

ACKNOWLEDGMENTS

We thank D. Durkin, D. Sayre, J. Kirz, B. Lai, and J. C. H. Spence for many stimulating discussions; B. Harteneck for the fabrication of the samples; Y. Nishino, Y. Kohmura, K. Tamasaku, and M. Yabashi for recording the diffraction patterns; P. Pianetta and B. Johnson for help in designing the apparatus; B. Lai, Z. Cai, and I. McNulty for the help of testing the apparatus; and G. Schneider and G. Denbeaux for imaging the samples by using the soft x-ray microscope at the Advanced Light Source. This work was supported by the U.S. Department of Energy, Office of Basic Energy Sciences. Additional support was provided by the U.S. DOE Office of Biological and Environmental Research and the National Institutes of Health. Use of the RIKEN beamline (BL29XUI) at SPring-8 was supported by RIKEN.

*Corresponding author. Electronic address: miao@ssrl.slac.stanford.edu

[1] D. Sayre, Acta Crystallogr. **5**, 843 (1952).
[2] R. P. Millane, J. Opt. Soc. Am. A **7**, 394 (1990).
[3] J. Miao, D. Sayre, and H. N. Chapman, J. Opt. Soc. Am. A **15**, 1662 (1998).
[4] J. Miao and D. Sayre, Acta Crystallogr., Sect. A: Found. Crystallogr. **56**, 596 (2000).
[5] J. Miao, P. Charalambous, J. Kirz, and D. Sayre, Nature (London) **400**, 342 (1999).
[6] I. K. Robinson, I. A. Vartanyants, G. J. Williams, M. A. Pferfer, and J. A. Pitney, Phys. Rev. Lett. **87**, 195505 (2001).
[7] I. A. Vartanyants and I. K. Robinson, J. Phys.: Condens. Matter **13**, 10593 (2001).
[8] J. Miao, K. O. Hodgson, and D. Sayre, Proc. Natl. Acad. Sci. U.S.A. **98**, 6641 (2001).
[9] J. Miao, T. Ishikawa, B. Johnson, E. H. Anderson, B. Lai, and K. O. Hodgson, Phys. Rev. Lett. **89**, 088303 (2002).
[10] J. Miao, K. O. Hodgson, T. Ishikawa, C. A. Larabell, M. A. LeGros, and Y. Nishino, Proc. Natl. Acad. Sci. U.S.A. **100**, 110 (2003).
[11] T. O. Mentes, C. Sánchez-Hanke, and C. C. Kao, J. Synchrotron Radiat. **9**, 90 (2002).
[12] U. Weierstall, Q. Chen, J. C. H. Spence, M. R. Howells, and R. R. Panepucci, Ultramicroscopy **90**, 171 (2002).
[13] J. Spence, U. Weierstall, and M. Howells, Philos. Trans. R. Soc. London, Ser. A **360**, 1 (2002).
[14] J. Miao, T. Ohsuna, O. Terasaki, K. O. Hodgson, and M. A. O'Keefe, Phys. Rev. Lett. **89**, 155502 (2002).
[15] A. Szöke, Acta Crystallogr., Sect. A: Found. Crystallogr. **57**, 586 (2001).
[16] R. Barakat and G. Newsam, J. Math. Phys. **25**, 3190 (1984).
[17] J. R. Fienup, Appl. Opt. **21**, 2758 (1982).
[18] D. Sayre, H. N. Chapman, and J. Miao, Acta Crystallogr., Sect. A: Found. Crystallogr. **54**, 233 (1998).
[19] K. A. Nugent, T. E. Gureyev, D. F. Cookson, D. Paganin, and Z. Barnea, Phys. Rev. Lett. **77**, 2961 (1996).
[20] K. Tamasaku, M. Yabashi, H. Yamazaki, N. Kawamura, M. Suzuki, and T. Ishikawa, Nucl. Instrum. Methods Phys. Res. A **467-468**, 686 (2001).
[21] We have found that the reconstruction is sensitive to the missing data at the center, which can be understood as follows. The oversampling method mainly relies on the constraint of the no-density region for the phase retrieval, in which a finite support (i.e., a boundary somewhat larger than the true envelope of the sample) is used to separate the electron density region from the no-density region. For a diffraction pattern with an area of missing data at the center, the lower spatial frequencies corresponding to the envelope of the sample are lost. During the process of the reconstruction, the algorithm keeps adjusting the values of the missing data to fit the defined finite support instead of the true envelope of the sample, which makes the reconstruction less effective. However, our simulations also showed that when the area of missing data is smaller than 10×10 pixels for a 2D diffraction pattern and $10\times10\times10$ voxels for a 3D diffraction pattern, the correct phases can usually be retrieved. These effects will be explored further in future studies.
[22] J. Kirz, C. Jacobsen, and M. Howells, Q. Rev. Biophys. **28**, 33 (1995).
[23] W. Meyer-Ilse, G. Denbreaux, L. E. Johnson, W. Bates, A. Lucero, and E. H. Anderson, in *X-Ray Microscopy*, edited by W. Meyer-Ilse, T. Warwick, and D. Attwood (American Institute of Physics, Melville, NY, 2000), pp. 129–134.
[24] The oversampling ratio of 5 may vary with the noise level in the diffraction patterns and the dimensionality of the samples. The process of reducing the sampling frequency by binning pixels may also increase the size of the oversampling ratio as it is actually needed.